RSC Advances

PAPER

View Article Online
View Journal | View Issue

Cite this: *RSC Adv.*, 2023, **13**, 8398

Chemically functionalized manufactured sand as the novel additive for enhancing the properties of cement-based composites

Jiangang Wo,[a] Di Wang,[b] Ting Zhang,[a] Chengfang Shi,[a] Zhengfa Zhou,[a] Aiguo Wang[b] and Wenping Wang *[a]

Received 18th January 2023
Accepted 6th March 2023

DOI: 10.1039/d3ra00373f

rsc.li/rsc-advances

The extensive applications of manufactured sand (AS) in cement-based composites were restricted because of its coarse surface texture, poor gradation and inevitable agglomeration. In this paper, a specifically designed polycarboxylate superplasticizer (PCE) decorated manufactured sand (AS-PCE) composite was synthesized *via* radical polymerization. The AS-PCE composite was characterized by FTIR, TGA, XPS and SEM. The load of PCE on the surface of AS was ~12 wt%. Our results show that AS-PCE can promote cement hydration reaction and refine the microstructure of a cement-based material, thus, reinforcing its mechanical strength. Meanwhile, the fluidity of cement mortar with 1 wt% AS-PCE particles was increased by 35% after 1 h hydration, due to the steric hindrance effect provided by polycarboxylate superplasticizer affiliated with AS-PCE. The AS-PCE can also significantly enhance the mechanical strength (especially, the flexural strength was about 25% increased after curing for 28 days) of mortar. The excellent improvements result from the synergistic effects of AS-PCE including superb dispersibility, promotion of cement hydration reaction and the repair of interfacial defects between AS particles and the cementitious material. The research provides a promising method for the AS application in cement-based materials.

1. Introduction

Cement-based composite materials are the most commonly used building materials in human society and have become an indispensable civil engineering material for construction infrastructures, such as bridges and buildings.[1–3] With the natural aggregate resource depletion and environmental pollution aggravating in the last few decades, currently, it is a hot topic to develop sustainable aggregates to replace natural aggregates. Apart from artificial geopolymer fine aggregates, manufactured sand also produced from crushing can be an alternative replacement of natural sand as well.[4–6] It is mentioned that such materials show a good suitability to produce strain-hardening cement-based materials. The manufactured sand usually produced from hard crushing rock depositions is generally more angular and has a rougher surface texture than natural aggregate, which always affects the workability of cementitious materials.[7–9] Normally, manufactured sand can enhance the compressive strength of concrete by increasing biting force between aggregates.[10] However, the concrete material tends to shrink and easily causes cracks under alkaline and low temperature conditions.[11] The coarse surface texture, poor gradation and agglomeration of manufactured sand always weaken the interfacial transition zones between the manufactured sand and other aggregates in concrete, which limits the reinforcing effect of manufactured sand on concrete material.[12,13] Consequently, the extensive application of manufactured sand in cement-based materials is restricted. As we know, the agglomeration and coarse surface of microfine can be weakened by incorporating some anionic surfactants, such as polyether-based superplasticizers, polycarboxylate, and polycarboxylate superplasticizers.[14,15]

The macromolecular polycarboxylate superplasticizers are comb-like polymers with a specific structure consisting of a backbone holding carboxy groups and pendant polyether chains.[16,17] It can not only adsorb the inorganic powders to keep the dispersion stable but also provide steric hindrance effects and electrostatic repulsion effects between the cement particles and other inorganic particles suspended in solutions, which can significantly improve the workability of cementitious materials without additional water, thereby optimizing rheological behavior to accelerate the degree of cement hydrothermal reaction.[18–20] The addition of polycarboxylate superplasticizers can provide a stress reduction in alkali-activated materials and also can improve the fluidity of fresh cement paste with stone powder.[21,22] However, the manufactured sand as an inorganic powder is difficult to keep

[a]*School of Chemistry and Chemical Engineering, Hefei University of Technology, Hefei 230009, China. E-mail: wwp65@sina.com*
[b]*School of Materials and Chemical Engineering, Anhui Jianzhu University, Hefei 230009, China*

compatible with superplasticizers by physical blending modification. The weak interaction between inorganic powders and superplasticizers cannot essentially solve secondary agglomeration in cement matrix materials.[23] Besides, the low adsorption efficiency between the powder and the modifier,[24] especially the impairment of PCE in alkaline medium,[15] is difficult to ensure the effective dispersion of inorganic powder in cementitious materials. And superfluous surfactants also may delay the hydration process and damage the mechanical performances of the mix.[25] Therefore, the surface of manufactured sand should be further modified to strengthen the bonding between manufactured sand and mortar or concrete matrixes, so as to improve the mechanical strength of cement matrix composites while keeping excellent workability. Numerous types of research have indicated that inorganic powders with decorated macromolecular superplasticizers can generate synergistic effects in cement-based materials, such as better dispersion stability,[26,27] excellent mechanical property,[28] and promotion of hydration,[29] which endows the cement-based composites with multiple superiorities. For example, S. H. Lv *et al.*[30] fabricated the graphene oxide nanosheet decorated by polycarboxylate to reinforce tough cement by copolymerization. Gu *et al.*[31] grafted shrinkage reducing admixture onto the surface of nano SiO_2 to increase the strength of cement paste at later ages. However, there has been surprisingly little research about manufactured sand as an additive to improve the property of cement-based materials. In this study, the macromolecular superplasticizers were grafted on the surface of manufactured sand. The obtained modified sand can not only serve as a supplementary cementitious material with excellent dispersity to fill the slight voids between the aggregate and cementitious material, but also act as an adhesion promoter to enhance the interactions between different aggregate particles, which can effectively enhance the mechanical strength of concrete material.

The chemical composition of the manufactured sand powder is comprised of silicate minerals and mainly made of silicon dioxide. As we know, piranha solution with strong oxidation capacity and high acidity is formed by a mixture of sulfuric acid and hydrogen peroxide by controlling their proportions, which usually was used to metal etching and clean organic pollutant from the surface of glassware and sintered glass.[32,33] Besides, the piranha solution also can create silanol groups on inorganic matter surface by modifying the surface structure of silicon dioxide building blocks.[34–36] The silanization of manufactured sand is influenced by the amounts and densities of hydroxyl group, due to the lack of hydroxyl groups on the outer layer of manufactured sand. Thus, we used the piranha solution to activate the manufactured sand surface. In this study, the surface of manufactured sand powder was functionalized by piranha solution to generate functional moieties (hydroxyl); then the silane coupling (KH570) with unsaturated bond was grafted on the surface of hydroxylated manufactured sand. Subsequently, the obtained composite (AS-PCE) was prepared by isoprenyloxy polyethylene glycol, acrylic acid, and 2-hydroxyl ethyl methacrylate phosphate. The comb-like macromolecular affiliating to AS-PCE can provide excellent dispersibility for the AS-PCE and cement particles because of the steric-hindrance effect. In the specific structure of the organic–inorganic hybrid, the water-soluble polymer introduced on the surface of manufactured sand can act as an adhesion promoter that enhanced the interactions between the modified sand and mortar or concrete matrixes, which can effectively improve mechanical properties, such as the bending strength and toughness of cement-based materials. Meanwhile, during the hydration process, the macromolecules on the modified sand surface can entangle the hydration products, further can prevent the generation and the development of microcracks in mortar or concrete composites. The AS-PCE composite material is expected to further promote the extensive application of manufactured sand serving as a fine aggregate in cement composites.

2. Experimental

2.1. Materials

Acrylic acid (AA, 98%), hydrogen peroxide solution (H_2O_2, 30%), 3-(methylacryloxy)propyltrimethoxysilane (KH570) and isoprenyloxy polyethylene glycol (TPEG, $M_w = 2400$) were grade products. Toluene, hydroquinone and ascorbic acid (VC) used in this study were all analytical reagents. 2-Hydroxyethyl methacrylate phosphate (HEMAP) was provided by Shanghai Aladdin Chemical Technology Ltd. Ordinary Portland cement (Po 42.5R) was provided by Anhui Conch Cement Co. Ltd. Manufactured sand which was passed from the 75 μm sieve and superplasticizer were provided by Anhui Tianqi Technology Co., Ltd.

2.2. Preparation process of AS-PCE

Firstly, the hydroxylated manufactured sand (AS-OH) powders were prepared by dispersing manufactured sand in a "piranha" solution (a mixture of H_2SO_4 and H_2O_2 at a 3 : 1 rate) for 4 h. Subsequently, the AS-OH powders were isolated by centrifugation, rinsed by water and placed in a vacuum drying oven at 50 °C overnight. Then, AS-OH (10 g), KH570 (10 g), hydroquinone (0.1 g) and toluene were put into a suitable three-point flask equipped with a magnetic stir bar and a condensing tube at 100 °C for 12 h (shown in Fig. 1(I)). Afterwards, the AS-KH570 was isolated by filtration and rinsed with ethanol. Finally, the obtained AS-KH570 was dried to remove moisture in a drying oven at 50 °C overnight.

The synthesis of modifier comb-PCE grafted onto the surface of manufactured sand involves detailed steps as follows (shown in Fig. 1(II)). Firstly, 20 g AS-KH570 was put into a three-necked flask. Beforehand, 20 g TPEG and distilled water were added into the flask. Then the above compound solution was vigorously stirred for 15 minutes, during when 0.24 g H_2O_2 was dropped. At the same time, solution A was obtained by blending 2.39 g AA, 0.7 g HEMAP and distilled water. Solution B was obtained by adding 0.12 g VC to the distilled water. Afterwards, the obtained solutions A and B were dropwise added into the above flask at room temperature *via* peristaltic pumps. The addition time of solutions was controlled about 2 h. When the addition was finished, the reactant was fully stirred for another

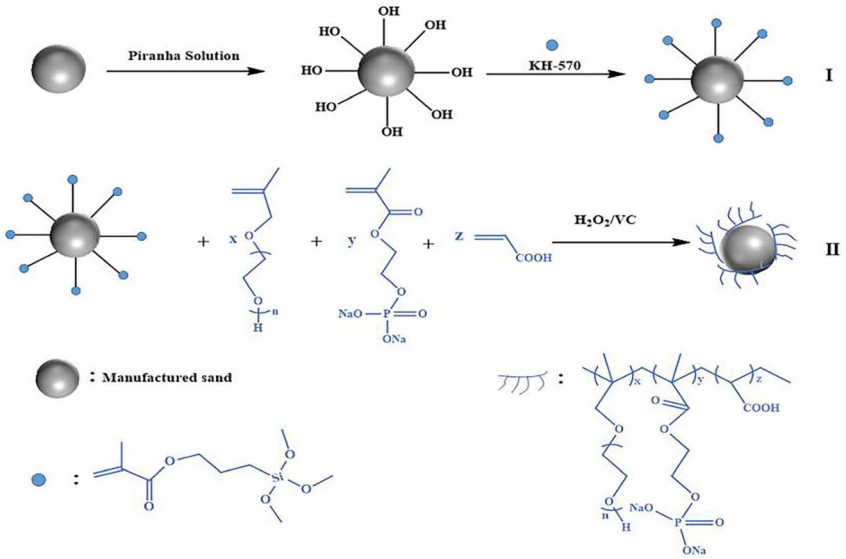

Fig. 1 Preparation process of manufactured sand coated with polycarboxylate superplasticizer.

3 h. Finally, the obtained product was separated by centrifugation, rinsed by distilled water, then placed in a vacuum drying oven at 60 °C for 24 h.

2.3. Preparation process of cement mortars and pastes

Cement mortars were prepared by mixing cement, water, manufactured sand (AS), modified sand (AS-PCE) and PCE according to Chinese standard GB 50119-2013, in which the AS-PCE accounted for 1%, 2%, 3%, 4% and 5% of manufactured sand by mass respectively. The sand was twice the mass of cement. The content of PCE in cement mortar is 0.3% of cement by mass. As shown in Table 1, the required water and PCE in preparation of the mortar without modified sand could be obtained when the mortar initial fluidity was controlled at 350 mm. The specific contents are shown in Table 1. According to the standard of GB/T 8077-2012 of China, water to cement ratio was controlled at 0.29 by mass in this research, in which the AS and AS-PCE accounted for 2% cement by mass respectively. The content of water reducer in mixture is 0.3% of binder by mass. The blending procedure is as follows: AS or AS-PCE, water and water reducer were put in stainless steel mixer together; then, cement was added into the above mixer at a rotation rate of 60 rpm. After 15 s interval, the obtained fresh cement paste was further stirred for additional 60 s at 500 rpm, then stirred for another 60 s at 1500 rpm.

Table 1 Mix design of different cement mortars

Cement	AS (g)	Water (g)	PCE	AS-PCE	Initial fluidity (mm)	1 h fluidity (mm)
600	1200	230	0.3%	0	350	260
600	1188	230	0.3%	12	370	350
600	1176	230	0.3%	24	372	355
600	1164	230	0.3%	36	375	360
720	1152	230	0.3%	48	376	362
720	1140	230	0.3%	60	380	365

2.4. Characterization

The samples were dried to remove moisture at 60 °C for 24 h. FT-IR spectrum was tested on a Nicolet spectrum analyzer by the method of KBr holder. The grafting ratio of superplasticizers on AS-PCE was analyzed by a simultaneous thermal analyzer (STA449F5, Jupiter, Germany) in the N_2 atmosphere from 20 °C to 800 °C at a heating rate of 10 °C min^{-1}. Furthermore, AS, AS-OH, AS-KH570 and AS-PCE were dried to constant weight in a drying oven at 50 °C for 24 h. X-ray photoelectron spectroscopy (XPS) was carried on a Thermo Scientific™ K-Alpha™+ spectrometer (amonochromatic Al Kα X-ray source (1486.6 eV) running at 100 W). Samples were measured under vacuum condition ($P < 10^{-8}$ mbar which equipped with a transmission energy of 150 eV (survey scans)). All sample peaks would be adjusted with C 1s peak, and its binding energy was at 284.7 eV for adventitious carbon. The detective peaks were all fitted with advantage software. The data was fitted by XPSPEAK software. The static surface water contact Angles of AS and AS-PCE were computed by automatic contact angle detector of Dataphysics OCA20 (Germany). The range of measurement is 0–180°, and the accuracy is ±0.1°. The SEM morphologies of AS and AS-PCE samples were obtained by Regulus 8230 high resolution field emission scanning electron microscope, and the acceleration voltage was about 20 kV.

2.5. Tests of cement pastes properties

X-ray diffraction (XRD) and resolution field emission scanning electron microscopy (SEM) were used to investigate the degree of cement pastes hydration process and microstructure. Three cement pastes (plain-cement sample, AS cement samples, AS-PCE cement samples) were prepared according to the above

cement paste mix design. Before test, these hardened pastes were put in ethanol overnight to cease the cement hydration process. Subsequently, the samples were dried out in a vacuum at 50 °C for 24 h to remove moisture. The cement pastes with AS, AS-PCE early heat of hydrations in cement were analyzed by isothermal calorimeter (TAM Air, US). Control the temperature of the samples store to 25 °C for 72 h.

2.6. Tests of cement mortars properties

The prismatic specimens (4 cm × 4 cm × 16 cm) for all cement mortars were cast and stored in plastic wraps at 25 °C. All the samples (totally 36 specimens were divided into two groups) were prepared by the proportions of Table 1, and carried out for the periods of 7 and 28 days measurements. After 24 h, the above cement mortars were demolded and subsequently cured under standard environment (humidity > 90%, temperature 20 ± 3 °C). The measurement is followed by the standard of the Chinese standard GB/T17671, the rate of loading for compressive strength was 2400 N s^{-1}, and the compressive and flexural strength in this research were the average values of three replicates. The toughness (three-point bending, 3PB) of the specimens (4 cm × 4 cm × 16 cm) were conducted using electronic universal testing machine (Model, CMT6103). The loading rate was set up to 0.02 mm min^{-1}, and the data collection frequency was 2 times per second. The distance between the centers of two fulcrums was 100 mm. All specimens were cured for 7 days under standard environment (humidity > 90%, temperature 20 ± 3 °C). The average value of the three samples in one group was regarded as the toughness of this group.

3. Result and discussion

3.1. AS-PCE characterization

The FT-IR spectra analysis was executed to confirm the subtle conversion of AS, AS-KH570, and AS-PCE in reaction process and the spectra was shown in Fig. 2(a). Obviously, the broad peaks at 1060 cm^{-1} resulted from the characteristic absorption peak of Si–O bond, and the broad peaks at 3390 cm^{-1} were ascribed to the stretching vibration of O–H. After reaction with KH-570, several distinct peaks emerged in the relative spectrum when compared with that of pristine AS. Peaks at 1412 and 1613 cm^{-1} could be ascribed to the bending vibration frequency of CH_2 and C=C, respectively. Besides, the other peak at 2917 cm^{-1} could be caused by the stretching vibration of CH_2. Upon treatment with polycarboxylate superplasticizer (PCE), the stretching vibrations at 1385 and 2920 cm^{-1} affiliating to AS-PCE became more intensive, resulting from that PCE which has a great abound of CH_2 has been grafted onto the AS surface. Furthermore, the characteristic peaks of AS-PCE also appeared at 1651 and 1720 cm^{-1} due to the grafting of C=C and COOH, which also demonstrates the excellent bonding of AS-PCE.

TG curves of AS, AS-OH, AS-KH570, and AS-PCE were analyzed by TGA, and the relative results were presented in Fig. 2(b). The curve of AS indicates a slight loss at 100–200 °C because of the removal of the absorbed water. The weight loss of

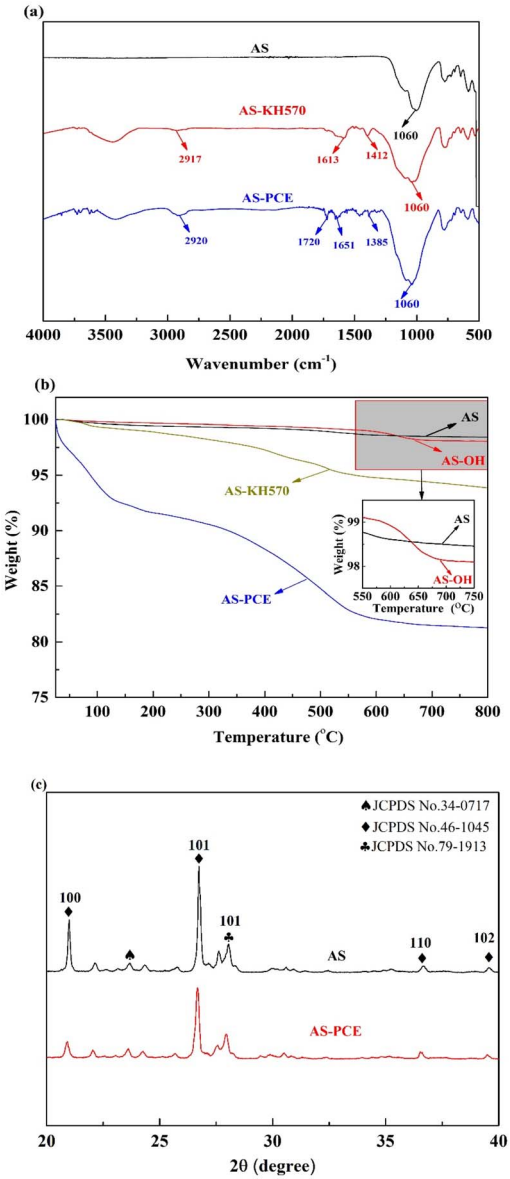

Fig. 2 (a) FTIR spectra of AS, AS-KH570 and AS-PCE; (b) TGA curves of AS, AS-KH570 and AS-PCE. Inset plots: the enlargement of AS and AS-OH; (c) XRD patterns of AS and AS-PCE.

the AS-OH was higher than pure manufactured sand (AS) ascribing to the numerous hydroxyl group enriched on the surface of AS-OH. While the relative weight loss of AS-KH570 resulted from the removal of the coupling agent on AS-KH570 composite surface. And the thermogravimetric curve of AS-PCE exhibited a remarkably higher weight loss compared with that of the AS-KH570, which implied that ~12 wt% PCE was efficiently coated onto the AS. The phenomenon above indicated that the grafting modification process of AS took place and the PCE polymerization has been successfully attached to the surface of AS, which is more beneficial to the performance of the composite material and a strong guarantee for good dispersion performance in the cement-based composites.

Fig. 2(c) shows the XRD patterns of pristine manufactured sand power and modified sand powder. The chemical composition of the manufactured sand powder is comprised of silicate minerals. As shown in Fig. 2(c), the manufactured sand used in this study is mainly made of three different crystalline forms of silicon dioxide. The samples indicated similar XRD spectrograms, showing that the crystalline structures of manufactured sand remain unchanged after graft modification. The peaks at 26.8° and 22.1° became weaker and the intensities of crystallization peaks decreased when compared with the pristine manufactured sand, indicating the phase of the manufactured sand was disturbed by the proximity of PCE.[37]

Surface analysis of the manufactured sand was carried out using X-ray photoelectron spectroscopy. The peaks at 102.77 eV, 149.3 eV, 285.2 eV and 532.46 eV belong to Si 2p, Si 2s, C 1s and O 1s on the manufactured sand surface, respectively. The curve in Fig. 3(a) which displays Si 2p, Si 2s and O 1s peaks can correspond to pristine manufactured sand components. Meanwhile, Fig. 3(b) and (c), display the XPS overlapping peaks of C 1s and O 1s scans on the AS-PCE, respectively. As shown in Fig. 3(b) C 1s of AS-PCE was fitted with three peaks at 284.7, 286.3, 288.5 eV,[38,39] which corresponds to the bond of C–C, C–OH and O–C=O, severally. And O 1s XPS spectra was fitted with two peaks at 532 eV (O–C=O) and 533.2 eV (C–OH),[40] respectively (±0.1 eV). Apparently, the AS-OH loaded with coupling reagent KH-570 can polymerizate with PCE, thus generating C–C bond in the AS-PCE structure, in which the obtained peak was concentrated at 284.7 eV. The appearance of C–OH and O–C=O components in Fig. 3(b) and (c), confirmed that the interaction between polycarboxylate superplasticizer and AS had successfully occurred.

The water absorption of manufactured sand is closely associated with the working performance of mortar and concrete materials. The surface wettability of pristine manufactured sand and the modified sand were shown in Fig. 4(a). The contact angle of pristine manufactured sand is almost 0°, which represents the high water absorption, because of its coarse surface texture and the rough edge and corner. After the PCE modification treatment, the contact angle became 26.9°, which indicates that the graft modification can reduce the water absorption. This may be due to the hydrophilic macromolecular polymer introduced on the surface of the modified manufactured sand, which provided steric hindrance from agglomeration. And, the smoother surface of modified manufactured with grafted superplasticizer can further reduce the adsorption of water. Thus, the graft modification process can effectively reduce the negative impact of the high water absorption on manufactured sand, which is conducive to enhancing the dispersing performance of cement-based materials.

Fig. 4(b) presents the SEM images of pristine sand and the modified sand, in which clusters and angular morphologies of pristine manufactured sands are observed. Whereas the image of AS-PCE hybrid particles shows that the AS-PCE has a much smaller particle size and better dispersion performance, and essentially smoother surface morphology. This implies that grafting modification decreases the surface energy of AS particles, thus avoiding the agglomeration due to manufactured sand powder and achieving a more uniform size.

3.2. Dispersing properties of AS/AS-PCE in alkaline conditions

Fig. 5(a) shows the peak absorbance values of UV-vis spectrometer for AS-PCE and AS with coincident concentration of 1 g/100 mL in pore, $Ca(OH)_2$, KOH and NaOH solutions with regard to time. Before the test, the above solutions were ultrasonically dispersed for 15 minutes. Significantly, the values of AS-PCE samples were evidently higher than the correlative values for AS samples in all instances. The relative results showed that the dispersion property of AS-PCE was better than that of AS in alkaline environment. Whereas the peak absorbance results of AS and AS-PCE were no remarkable difference in the $Ca(OH)_2$ solutions. This can be due to the reduction of the steric hindrance effect provided PCE as a result of calcium-crosslinking with carboxy and phosphate affiliating to AS-PCE. Unlike the AS solutions, in which initial agglomerations were observed, no immediate agglomerations for AS-PCE solutions were detected upon its addition into the above solutions in Fig. 5(b). During the first 60 min, the values of absorbance decreased, relating to the deposition of AS and AS-PCE in the cuvettes. At 1 h after shaking the solutions, the absorbance of AS-PCE can be greatly recovered than that of AS. The better

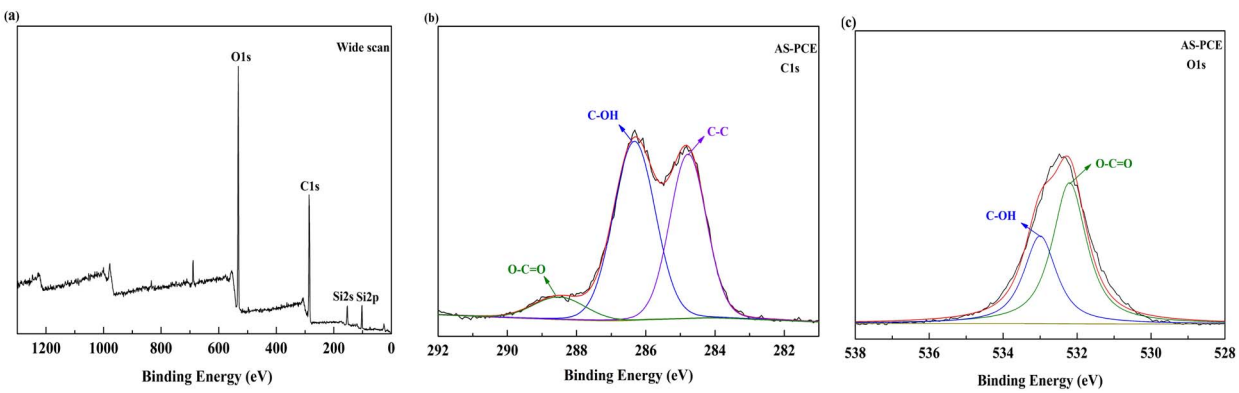

Fig. 3 The XPS survey spectra: (a) wide scan, (b) C 1s (narrow scan), and (c) O 1s (narrow scan) of AS-PCE.

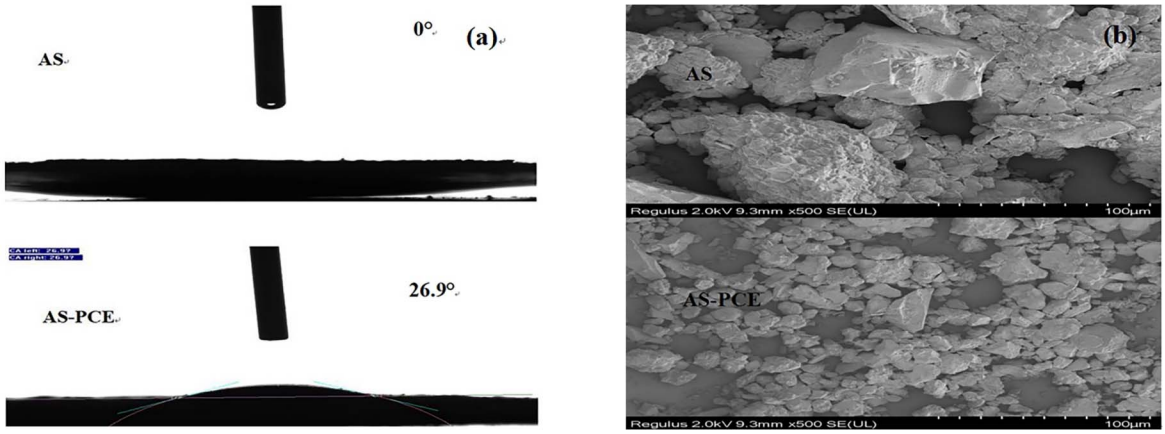

Fig. 4 (a) The contact angles of AS and AS-PCE; (b) SEM images of AS and AS-PCE.

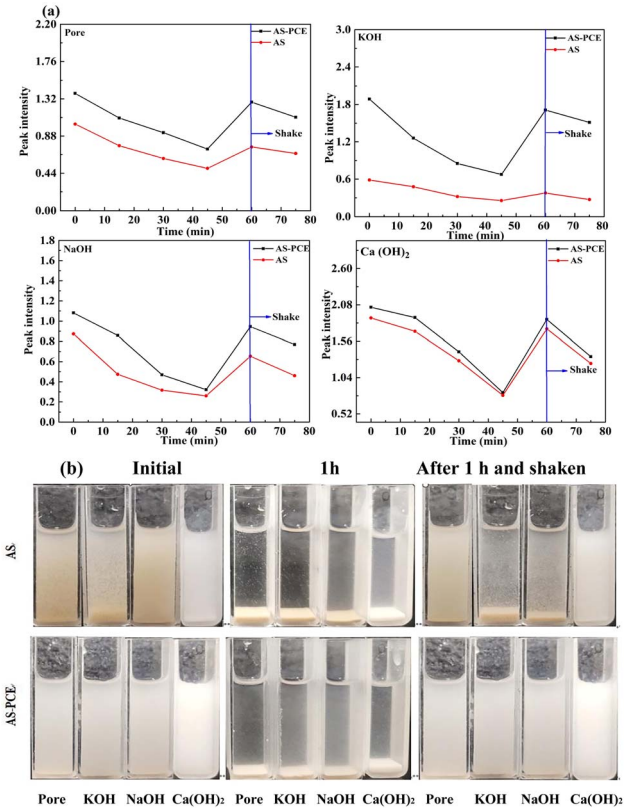

Fig. 5 (a) Peak absorbance of AS/AS-PCE in pore, KOH, NaOH and $Ca(OH)_2$ solutions; (b) visual observation of AS/AS-PCE dispersion in different solutions were captured at t = 0 min, 1 h and 1 h with immediate shake, respectively.

dispersity and stability of AS-PCE in alkaline environments were because of the structure of macromolecular chain coating on AS-PCE which provides steric hindrance and some Pore KOH NaOH $Ca(OH)_2$ Pore KOH NaOH $Ca(OH)_2$ Pore KOH NaOH $Ca(OH)_2$ functional groups. The synergistic function of hindrance effects and hydrolysis of ester group in alkaline environment guaranteed superb dispersion. The results above mean during the initial and 60 min mixture procedure, AS-PCE can be well dispersed in cement matrix, which guarantees the excellent workability of cement-based materials.

3.3. Workability

Proverbially, the excellent workability is an essential indicator to guarantee the homogeneity of the cement matrix composites. Nevertheless, the inclusion of pristine AS with a much rough surface texture in cement-based materials demanded additional water to moisten the coarse surface and seriously decreased the fluidity, leading to the increase of viscosity and porosity. In this research, the fluidity of fresh mortars at different AS-PCE dosages replacing AS was assessed using a "mini-slump" measurement. The results about initial and 1 h fluidities were presented in Fig. 6. The mortar without AS-PCE presented poor fluidity. The reason is that the manufactured sand as an inorganic powder is difficult to keep compatible with superplasticizers by physical modification. And the weak interaction between the pristine sand and superplasticizer cannot essentially solve secondary agglomeration and poor gradation of manufactured sand. As expected, it can be clearly observed that

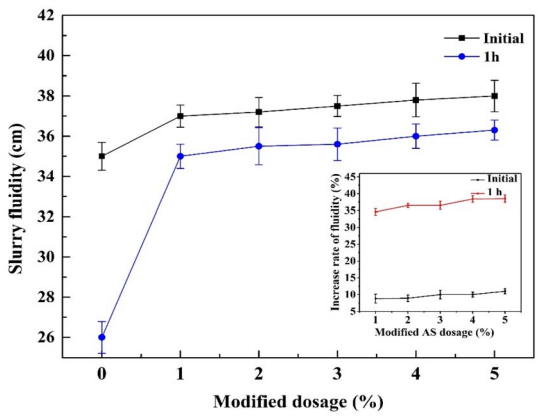

Fig. 6 Effects of AS-PCE on cement mortar initial and 1 h fluidities. Inset plot: the increase rate of mortar fluidity.

the initial and 1 h slurry fluidities of mortars gradually increased with the adulteration of AS-PCE. The fluidity of cement mortar with 1 wt% AS-PCE particles was increased by 35% after 1 h hydration. The carboxylic and phosphate groups in PCE structure grafted on the manufactured sand surface can be served as adsorption groups to improve the adsorption capacity, hence the dispersing performance of modified sand for mortar materials can be enhanced. And, the large molecular polyether chains coated on AS-PCE also provided a larger steric hindrance, through which the agglomeration of the inorganic powder was weakened. Meanwhile, the water-soluble polymers on the surface of AS-PCE also can better disperse cement particles, causing better fresh cement mortars fluidity. After 1 h hydration, compared with the samples without AS-PCE, the fluidity with AS-PCE had increased by ~35% only at a dosage of 1% wt of AS, and the fluidity also increased gradually with the increase of AS-PCE. The reason is sufficient anionic groups have been introduced to the surface of modified sand and increased the negative charge density, thus the electrostatic repulsive dispersion between cement particles and the modified sand can be increased. Besides, the interaction between PCE and manufactured sand was stronger by the formation of chemical bonds, and the secondary agglomeration in powders was difficult to occur, causing better slurry fluidity retention behavior. Finally, the hydrolysis of ester group on the surface of AS-PCE in alkaline environment also can effectively postpone the loss of fluidity, which could explain why AS-PCE doped in cement mortar exhibited excellent slurry fluidity than plain mortar.

3.4. Hydration process

The XRD characterizations for Blank, AS and AS-PCE hardened cement paste samples after curing 3 and 7 days were presented in Fig. 7. As shown in Fig. 7(a), it can be significantly noted that the lower relative peak intensities of unhydrated C_2S and C_3S in samples containing AS-PCE with respect to the samples containing AS and blank samples indicated a higher hydration degree of cement paste. Besides, the CH peak intensities of all samples decreased gradually as a function of the hydrated period when hydrated for a consistent period. The hydrated product C–S–H gels were always amorphous because of the inherently poor crystallinity.[31] Thus, it is difficult to distinguish the diffraction peaks of C–S–H on the XRD pattern. Ghafari[41] and Kim[42] thought the cement hydration and pozzolanic effect can be measured by the variations of CH peak intensity. The crystal planes (001), (011) and (012) homologous to the three angles of CH hydration products at 18.2°, 34.2° and 47.3° were chosen to calculate the crystal size of CH.[43] The crystal size of CH can be calculated by the Scherrer equation:[44]

$$D = \frac{K\gamma}{B\cos\theta}.$$

where D is the crystal size corresponding to the crystal plane, γ is the wavelength of incident X-ray ($\gamma = 0.15406$), θ represents the relative diffraction angle from the incident X-ray to the crystal plane, B represents the half-height-width (FWHM) of the diffraction peak value, and K equals to constant 0.89. Fig. 7(b) indicates the crystal size of CH. It is obviously observed that the crystal sizes of CH on (001), (011) and (012) planes present the results of AS > Blank > AS-PCE crystal after curing for 3 and 7 days. The results show that the manufactured sand modified by PCE made the crystal size of $Ca(OH)_2$ smaller, indicating the adequate hydration reaction. The inadequate pozzolanic reaction in AS cement paste could be attributed to the bad incompatibility of AS with cement particles and the decrease of cement dispersion in the system. After the PCE modification of AS, the peripheral polymer shell can provide some functional groups, such as carboxyl and phosphate, to react with calcium hydroxide, meanwhile, the polymer grafted on AS-PCE is interspersed in the whole system, causing the obvious improvement of cement dispersion in the system, thus, the higher degree of the pozzolanic reaction occurred between the modified sand and the cement matrix.

Fig. 8 shows the influence of the inclusion of AS and AS-PCE particles on the hydration process of cement pastes with 2% replacement dosage by mass of solids. The result shown in Fig. 8(a) displays that AS particles slowed down the cement hydration at the first one hour. The reason why the hydration reaction was delayed is that the rough surface of pristine manufactured sand absorbed the water in the system. Compared to the paste with the same addition of AS particles, the paste incorporating AS-PCE presented a longer hydration process at the first one hour. This reason is polymer chains introduced on the modified manufactured sand were adsorbed on the surface of AFt covering layers with positive charges, which hinders the transmission of SO_4^{2-}, thus delaying the formation of AFm.[45] Besides, the water-soluble polymers with multi-branched held the water layers adsorbed on the surface of the modified sand, which is conducive to the retention of water and hinders the release of water, thereby delaying the cement hydration process. And, the reason why the paste with AS particles tended to have the minimum cumulative heat in all

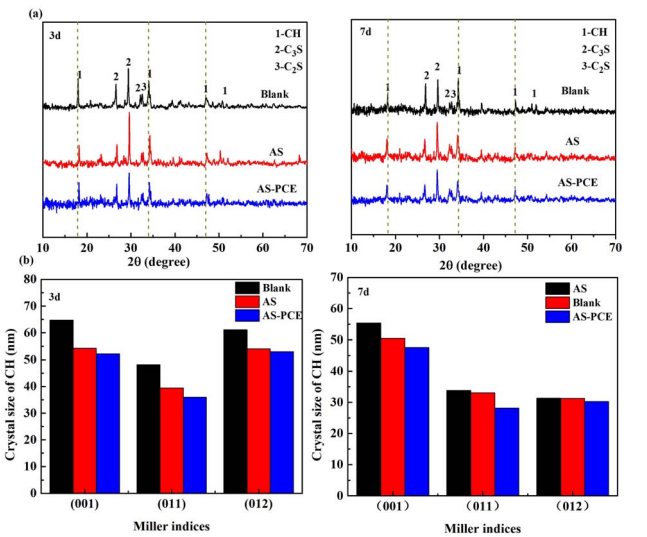

Fig. 7 (a) XRD patterns of hardened cement pastes with AS and AS-PCE; (b) their crystal sizes of CH at different Miller index in XRD after curing for 3 and 7 days respectively.

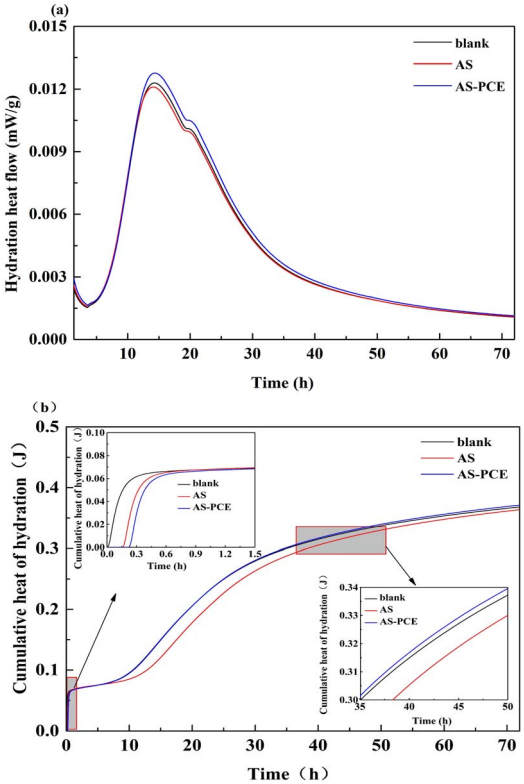

Fig. 8 Air isothermal calorimeter measurement of (a) heat flow and, (b) cumulative heat of hydration. Inset plot: the enlargement of cumulative heat hydration of cement.

cases is that the cement components involved in the hydration reaction were reduced when the manufactured sand partially replaced the cement. From Fig. 8(b), it can be found that the relative hydration heat release intensively happened at the first 35 h. Then it increased slowly until the cumulative heat became stable. Compared with another two samples, the paste containing AS-PCE had the largest heat flow peak value and cumulative heat of hydration. As for the influence mechanism of fine powder on the cement hydration behavior, it is generally believed that the promotion effect of fine powder on early cement hydration mainly lies in nucleation effect, which reduces the nucleation barrier and provides more nucleation sites for the growth of hydration products.[46,47] The modified manufactured sand with smoother surface and excellent dispersibility can reduce the absorption of water, which avoids the adverse effect on cement hydration reaction. The polycarboxylate superplasticizer which anchored on manufactured sand surface can make the particles more stable and better dispersed in cementitious environment than pristine sand. The AS-PCE with lower degree of agglomeration size would have space to fill in. Consequently, the modified sand can provide additional surface areas for the growth of hydration products and the nucleation effect can be more produced. The largest heat flow and cumulative heat curves of the AS-PCE sample indicate the addition of modified manufactured sand is conducive to the hydration of cement paste.

3.5. Microstructure

The microstructures of early hydrated cement products with AS and AS-PCE were investigated using scanning electron microscopy (SEM) at different magnifications. The results presented in Fig. 9 reveal the hydrated cement productions mixed with AS and AS-PCE at 3 and 7 days. After curing 3 and 7 days, Fig. 9(c) and (d) show the microstructures of the AS hardened cement paste with loose structures and amounts of microcracks. Due to the inadequate hydration of the AS-cement sample, large amounts of needle-like crystal products appeared in the system. It can be observed that a great number of obvious transition zones incorporating porosity and pore size distribution appeared between hydration products and AS. However, Fig. 9(a) and (b) show that the hydrated cement products mixing with AS-PCE formed compacted microstructures. The interweaving and cross-linking microstructures caused fewer microstructures to occur in the system. With the process of hydration, the surface of AS-PCE has been coated with cement hydration products, so the hydrated cement products can bind to the AS-PCE more firmly. And fewer formations of ettringite precipitating at the cement hydration process can promote the AS-PCE-cement early-age hydration. Moreover, AS-PCE with smaller particle size distribution can fill in the interstice of hydrated cement products, and interlaced with acicular ettringite, which forms the reticulate structure between transition zones. This is due to the fact that the polycarboxylate superplasticizers were chemically bonded to the AS-PCE surface, which increases the interactions between manufactured sand particles and the cementitious material. Therefore, the whole system presents a continuous dense structure.

3.6. Mechanical behavior of cement mortars with AS-PCE

The toughness of cement-based materials is an essential guarantee for their applications in engineering. In this study, the toughness of mortars with modified sand was characterized by bending strength. Fig. 10 indicates the experimental stress–strain curves of the mortars with doping different additions of AS-PCE. The toughness of doping the modified sand became higher, and the mortar with 2% AS-PCE had the best bending strength. Possible reasons are (a) the filling effect of AS-PCE particles, (b) the macromolecular superplasticizer coated on the modified sand surface can crosslink with hydration products, (c) AS-PCE caused the improvement of cement particles dispersion, which makes the sufficient hydration reaction. However, adding more modified sand will cause a decrease in strength. The reason is the superfluous macromolecular network structure on AS-PCE absorbed and constrained the free water reducer or cement particles, impeding the hydration of cement and impairing the enhancement of AS-PCE on toughness.

The impact of AS-PCE in cement mortar on the variation in compressive and flexural strengths at 7 and 28 days was studied respectively. The curves of mechanical strength of mortar in Fig. 11(a) and (b) present first an increase and then decrease trend with the increase in AS-PCE replacement level. All the mechanical strength increased to the maximum value with the

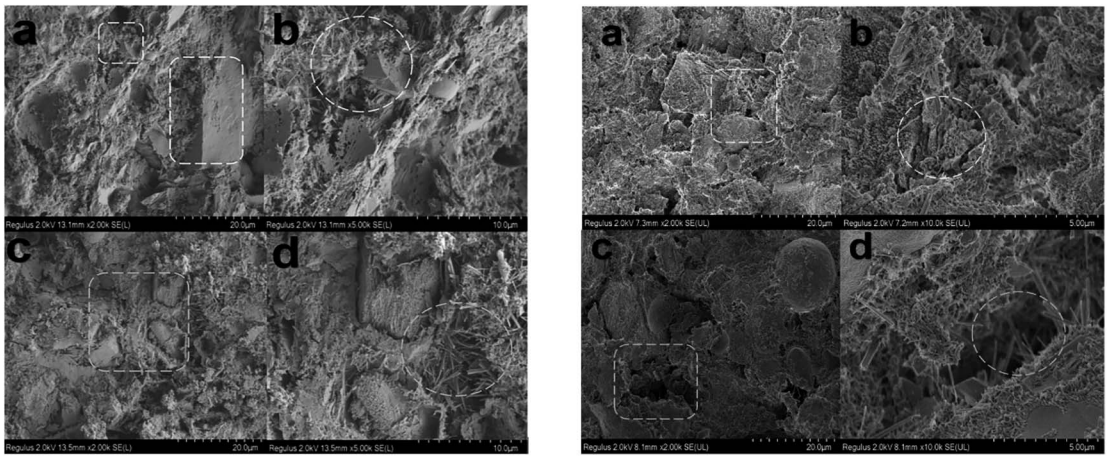

Fig. 9 SEM images of the microstructure of hydrated cement pastes: (a and b) AS-PCE hardened cement pastes and (c and d) AS hardened cement pastes at 3 and 7 curing days, respectively.

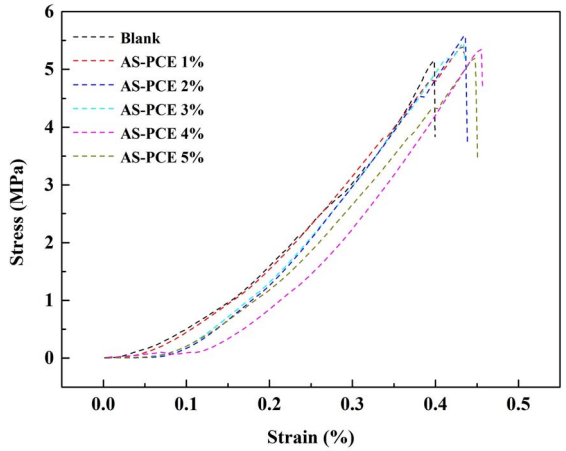

Fig. 10 Stress–strain curves of the mortars with modified sand.

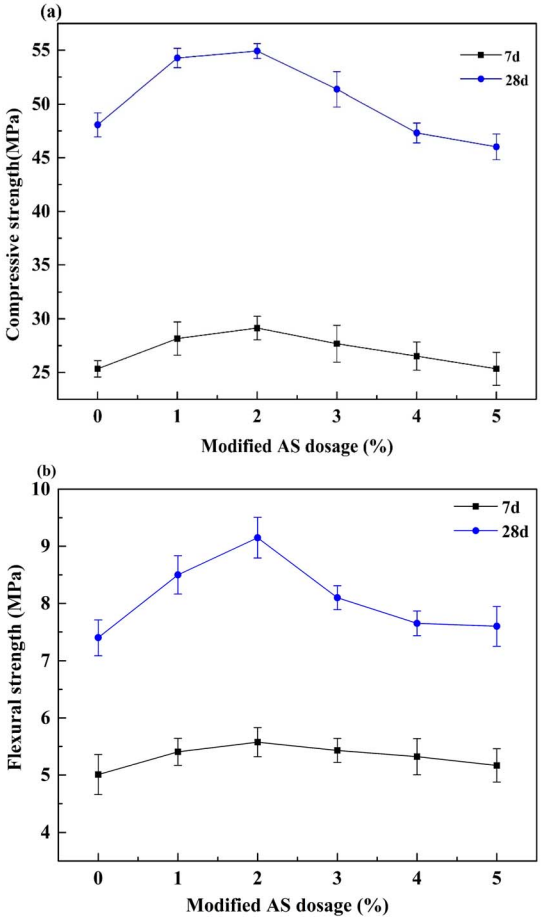

Fig. 11 (a) Compressive and (b) flexural strength evolution of the mortars with AS-PCE.

dosage of AS-PCE being 2%. And, the mortar compressive strength increased by 9% and the flexural strength increased by 25%. The improved strength of mortar with AS-PCE can be attributed to refined microstructure and excellent interfacial. The bulky molecular structures of the PCE grafted on manufactured sand surface could provide additional steric repulsion, which can prevent the early aggregation of AS-PCE particles. Compared with the sample without AS-PCE samples, the proposed de-aggregation functionality endowed by PCE also can enable AS-PCE particles to enter microcracks and pack pores more closely in cement-based materials. The graft modification of manufactured sand with PCE makes the AS-PCE particles disperse better in cement-based materials. This can provide additional nucleation for C–S–H. Besides, abundant carboxyl, phosphate introduced into the surface of AS-PCE can combine with calcium ions in cement in the form of ionic bond, which can improve aggregate interface properties and increase the bonding force between the modified sand and cement-based materials, which could explain why the mortar with AS-PCE can exhibit higher strength than plain samples. Moreover, the polymer grafted on the surface of AS was interspersed in the whole structures, which can tightly adhere to the cement hydration products and achieve stronger bonding force in the system. It prevented the generation and expansion of microcracks in the hardened cement mortar materials, increasing the

toughness and flexural strength of the cement-based composite materials. But, it can be observed that no further increase in mechanical strengths occurred once the content of AS-PCE reaches 2%. The reason is that the superfluous macromolecular network structure on the surface of AS-PCE absorbed and constrained the polycarboxylate superplasticizer or cement particles, reducing the dispersion of polycarboxylate superplasticizer and impeding the hydration of cement, which weakens the strengthening effects of AS-PCE on cement mortar materials.

4. Conclusion

In this study, a specifically designed polycarboxylate decorated manufactured sand (AS-PCE) composite was synthesized *via* radical polymerization. TG curves indicated that the load of water reducer on AS-PCE surface was ~12 wt% by chemical bond. Moreover, AS-PCE incorporated in the cement-based materials prevented manufactured sand particles and cement particles from agglomerating by exhibiting strong steric hindrance effects of PCE's macromolecular branched chains. The fluidity of mortar significantly improved with the increase of AS-PCE, and the collapse resistance of cement mortar with 1 wt% modified sand increased by nearly 35% after 1 h hydration. The addition of AS-PCE can promote the cement hydration reaction and increase the release of hydration heat. The AS-PCE with better dispersibility can provide additional nucleation for hydration products. Meanwhile, the excellent dispersion of AS-PCE caused the obvious improvement of cement dispersion in the system, which makes the cement hydration reaction more sufficient. With AS-PCE addition, the toughness also can be enhanced. Improved mechanical performance with AS-PCE was confirmed by a 9% increase in mortar compressive strength and a 25% increase in mortar flexural strength, when compared to the control samples without AS-PCE after curing for 28 days. The reason is the modified sand can be stacked more closely in cement-based materials owing to its excellent dispersibility. Meanwhile, the interweaving and cross-linking microstructures of [AS-PCE-CSH] prevented the generation and expansion of microcracks in the hardened cement paste, which increases the toughness and flexural strength of the cement-based materials. The research provides a promising method for the AS extensive application in cement-based composite materials.

Author contributions

Jiangang Wo: methodology, formal analysis, investigation, writing – original draft. Di Wang, Aiguo Wang: formal analysis, writing – review & editing. Ting Zhang, Chengfang Shi and Zhengfa Zhou: methodology, supervision. Wenping Wang: conceptualization, funding acquisition, project administration.

Conflicts of interest

The authors declare that they have no known competing financial interests or personal relationships that could have appeared to influence the work reported in this paper.

Acknowledgements

The authors would like to acknowledge the Natural Science Foundation of China (No. 2013GJMS0526, 52003004 and 51372059) for the financial support.

Notes and references

1 D. D. L. Chung, *J. Mater. Sci.*, 2004, **39**, 2973–2978.
2 Y. Zhang, S. Wang, B. Zhang, D. Hou, H. Li, L. Li and C. Lin, *Constr. Build. Mater.*, 2020, **237**, 117501.
3 C. Zhang, J. Fu, J. Yang, X. Ou, X. Ye and Y. Zhang, *Constr. Build. Mater.*, 2018, **187**, 327–338.
4 L. Y. Xu, B. T. Huang and V. C. Li, *Cem. Concr. Compos.*, 2022, **125**, 104296.
5 L. Y. Xu, B. T. Huang, Q. Lan-Ping and J. G. Dai, *Cem. Concr. Compos.*, 2022, **133**, 104676.
6 S. Singh, R. Nagar and V. Agrawal, *J. Clean. Prod.*, 2016, **126**, 74–87.
7 Z. Ma, J. Shen, C. Wang and H. Wu, *Cem. Concr. Compos.*, 2022, **132**, 104629.
8 W. Shen, Z. Yang, L. Cao, Y. Liu and H. Yang, *Cem. Concr. Compos.*, 2016, **114**, 595–601.
9 G. G. Cho, J. Dodds and J. C. Santamarina, *J. Geotech. Geoenviron.*, 2006, **132**, 591–602.
10 B. Li, J. Wang and M. Zhou, *Constr. Build. Mater.*, 2009, **23**, 2846–2850.
11 F. Zhou, G. Pan and L. Zhang, *J. Build. Eng.*, 2023, **63**, 105542.
12 C. F. Goble and M. D. Cohen, *ACI Mater. J.*, 1999, **96**, 657–662.
13 D. D. Cortes, H. K. Kim, A. M. Palomino and J. C. Santamarina, *Cem. Concr. Res.*, 2008, **38**, 1142–1147.
14 Y. Sargam, K. Wang, A. Tsyrenova, F. Liu and S. Jiang, *Cem. Concr. Res.*, 2021, **144**, 106417.
15 A. Javadi, T. Jamil, E. Abouzari-Lotf, M. D. Soucek and H. Heinz, *ACS. Sustainable Chem. Eng.*, 2021, **9**, 8354–8371.
16 J. Plank and M. Gretz, *Colloids Surf., A*, 2008, **330**, 227–233.
17 H. Uchikawa, S. Hanehara and D. Sawaki, *Cem. Concr. Res.*, 1997, **27**, 37–50.
18 R. J. Flatt and Y. F. Houst, *Constr. Build. Mater.*, 2001, **31**, 1169–1176.
19 D. Jansen, F. Goetz-Neunhoeffer, J. Neubauer, R. Haerzschel and W. D. Hergeth, *Cem. Concr. Compos.*, 2013, **35**, 71–77.
20 F. Winnefeld, S. Becker, J. Pakusch and T. Götz, *Cem. Concr. Compos.*, 2007, **29**, 251–262.
21 A. Kashani, J. L. Provis, J. Xu, A. R. Kilcullen, G. G. Qiao and J. S. Van, *J. Mater. Sci.*, 2014, **49**, 2761–2772.
22 H. Feng, L. Pan, Q. Zheng, J. Li, N. Xu and S. Pang, *Constr. Build. Mater.*, 2018, **170**, 182–192.
23 S. Mallakpour and M. Naghdi, *Prog. Mater. Sci.*, 2018, **97**, 409–447.
24 F. Collins, J. Lambert and W. H. Duan, *Constr. Build. Mater.*, 2012, **34**, 201–207.
25 H. Du and S. D. Pang, *Cem. Concr. Compos.*, 2015, **76**, 10–19.
26 B. Liu, L. Wang and G. Pan, *J. Build. Eng.*, 2022, **57**, 104860.
27 M. Wang and H. Yao, *Materials*, 2020, **13**, 3385.

28 G. Wang, H. Tan and J. Zhu, *Constr. Build. Mater.*, 2022, **328**, 127032.
29 P. Feng, H. Chang and X. Liu, *Mater. Des.*, 2020, **186**, 108320.
30 S. H. Lv, L. J. Deng, W. Q. Yang, Q. F. Zhou and Y. Y. Cui, *Cem. Concr. Compos.*, 2016, **66**, 1–9.
31 Y. Gu, Z. Wei, Q. Ran, X. Shu, K. Lv and J. Liu, *Cem. Concr. Compos.*, 2017, **75**, 30–37.
32 J. Singh, A. Mehta, M. Rawat and S. Basu, *J. Environ. Chem. Eng.*, 2018, **215**, 121–124.
33 L. He, F. Lin, X. Li, Z. Xu and H. Sui, *J. Environ. Chem. Eng.*, 2016, **4**, 1753–1758.
34 J. Escorihuela and H. Zuilhof, *J. Am. Chem. Soc.*, 2017, **139**, 5870–5876.
35 D. S. Carretero, C. P. Huang and J. H. Tzeng, *J. Hazard. Mater.*, 2021, **406**, 124658.
36 P. Sun, G. Liu, D. Lv, X. Dong, J. Wu and D. Wang, *RSC Adv.*, 2015, **5**, 52916–52925.
37 L. Feng, Y. Wang, N. Wang and Y. Ma, *Polym. Bull.*, 2009, **63**, 313–327.
38 R. Al-Gaashani, A. Najjar, Y. Zakaria, S. Mansour and M. A. Atieh, *Ceram. Int.*, 2019, **45**, 14439–14448.
39 R. Muzyka, S. Drewniak, T. Pustelny, M. Sajdak and L. Drewniak, *Materials*, 2021, **14**, 769–782.
40 C. Y. Lee, J. H. Bae, T. Y. Kim, S. H. Chang and S. Y. Kim, *Composities, Part A*, 2015, **75**, 11–17.
41 K. M. Kim, Y. S. Heo, S. P. Kang and J. Lee, *Cem. Concr. Compos.*, 2014, **49**, 84–91.
42 U. Holzwarth and N. Gibson, *Nat. Nanotechnol.*, 2011, **6**, 534.
43 H. Wang, P. Li and D. Yu, *Nano. Lett.*, 2018, **18**, 3344–3351.
44 H. Minard, S. Garrault, L. Regnaud and A. Nonat, *Cem. Concr. Res.*, 2007, **37**, 1418–1426.
45 J. J. Thomas, H. M. Jennings and J. J. Chen, *J. Mater. Sci.*, 2009, **113**, 4327–4334.
46 A. M. Poppe and G. D. Schutter, *Cem. Concr. Res.*, 2005, **35**, 2290–2299.
47 B. Lothenbach, G. L. Saout, E. Gallucci and K. Scrivener, *Cem. Concr. Res.*, 2008, **38**, 848–860.